Proceedings of ACTIVE 99, International Symposium on Active Control of Sound and Vibration, Ed. Scott Douglas, pp. 1193–1204, Fort Lauderdale, Florida, 2-4 December 1999

A MAGNETOELASTIC MODEL FOR MAGNETOSTRICTIVE SENSORS

Marcelo J. Dapino,[a] Frederick T. Calkins,[b] Ralph C. Smith[c] and Alison B. Flatau[d]

a,d AEEM Department, Iowa State University, Ames, IA 50011
b Boeing Phantom Works, Seattle, WA 98136
c CRSC, Department of Mathematics, North Carolina State University, Raleigh, NC 27695

INTRODUCTION

The interest in sensor technologies has grown considerably in recent years, due to the increasingly important role that sensors play in sectors such as the aerospace, automotive and manufacturing industries [1]. The high energy coupling factors of up to $k \approx 0.76$ achieved with certain magnetostrictive materials motivates the utilization of these materials in sensing applications involving energy conversion between the mechanical and magnetic states. Of particular interest are the highly magnetostrictive rare earth-iron compounds R-Fe_2 (R = Tb, Dy, Ho, Sm), of which at present Terfenol-D is the most well known commercially available example.

A magnetostrictive transducer is here defined as a *device* which employs a magnetostrictive material to convert between mechanical and magnetic energies. It is emphasized that this energy exchange is bidirectional, that is both transduction processes (magnetic to elastic and elastic to magnetic) occur simultaneously during operation. In actuation mode, the action of a magnetic field and ensuing magnetization changes generates strains and forces in the magnetostrictive material. In sensing mode, the application of forces creates substantial magnetization changes which can be detected in a variety of ways. Both modes of operation are intrinsically coupled, and hence a mechanism capable of addressing this coupling must be considered in models to be used in design and control of magnetostrictive devices. In addition to providing actuation and sensing capabilities, magnetostrictive materials are mechanically robust (when operated in compression), they do not exhibit fatigue as other transducer technologies do, they are not frequency-limited and their properties can be widely modified through both stoichiometric modifications and changes in operating conditions.

Some of the earliest examples of the use of magnetostrictive materials in sensor applications included the telephone receiver, hydrophone, and scanning sonar [2]. More recent sensor designs include hearing aids, load cells, force transducers, accelerometers, proximity sensors, torque sensors, magnetometers, and frost detectors [3]. Many of these devices rely on the Villari effect, which has been the subject of extensive research [3, 4]. Other uses involve the utilization of both the actuation and sensing modes simultaneously, such as in the simultaneous sensing and control of structural vibrations in acoustical systems [5, 6].

While magnetostrictive transducers provide adequate performance at the low signal levels where their behavior is quasilinear (magnetostrictions below $\lambda_s/3$), the demand for high performance transducers often dictates that they be driven at the high operating regimes where hysteresis and nonlinearities are intrinsic to magnetostrictive performance. In addition, the advantages of magnetostrictive materials over alternative transducer technologies are typically realized at high operating regimes. These factors motivate the development of models that accurately characterize the hysteresis, nonlinearities and coupling effects intrinsic to magnetostrictive transduction.

Material models based on the linear piezomagnetic equations are being extensively used to quantify magnetostrictive transducer performance. These models are typically formulated as follows,

$$\varepsilon = s^H \sigma + d_{33} H \tag{1}$$

$$B = d_{33}^* \sigma + \mu^\sigma H. \tag{2}$$

In these equations, ε is the strain, s^H is the compliance at constant applied magnetic field H, d_{33} and d_{33}^* are the magnetoelastic coupling coefficients, σ is the stress, and μ^σ is the permeability at constant stress. It is emphasized that this model is in essence a generalization of two phenomenological relationships, namely the Hooke's law for linearly elastic solids $\varepsilon = s\sigma$ and the magnetic constitutive equation $B = \mu H$. The total magnetoelastic strain ε given by equation (1) is interpreted as the superposition of the elastic or passive response $\varepsilon \equiv s\sigma$ and the magnetostrictive component $\lambda \equiv d_{33} H$ associated with domain processes in the material. In a similar fashion, the magnetic induction B of equation (2) is interpreted as due to the constant-stress magnetic component $\mu^\sigma H$, and a term due to magnetoelastic interactions $d_{33}^* \sigma$. It is often assumed on the basis of small reversible magnetostrictions that $d_{33}^* = d_{33}$, which suggests that, for reversible processes, a large magnetomechanical effect $d_{33}^* \equiv (\partial B / \partial \sigma)_H$ should be observed in materials with large axial strain coefficient $d_{33} \equiv (\partial \varepsilon / \partial H)_\sigma$.

A related modeling approach has been reported in [7]. This experimentally verified model quantifies the output produced by a velocity sensor consisting of a magnetically biased Terfenol-D core. The sensor is connected to a moving target that strains the core producing a change in magnetic induction. The linear constitutive equations, Faraday-Lenz law, and empirical fits relate the transducers open circuit output voltage to the target velocity. Kleinke and Uras describe the single branch sensor model (SBSM) for magnetostrictive force sensors [8]. An applied force on the sensor causes a strain in a magnetostrictive element. The magnetomechanical relationship between the mechanical strain and magnetic circuit reluctance, measured by a receiving coil, is modeled by a two dimensional magnetic moment rotation. Models have also been developed for a noncontact torque sensor [9] and a magnetometer [10, 11].

While the linear piezomagnetic model (1)-(2) and related modeling techniques provide adequate characterization of magnetostrictive performance in quasilinear regimes, general models and corresponding numerical methods appropriate for characterizing transducer nonlinearities, coupling effects and hysteresis losses are still lacking. To address this problem, a nonlinear and hysteretic magnetomechanical model for the strains and forces generated by magnetostrictive transducers in response to applied magnetic fields was presented in [12, 13, 14]. The model was employed to characterize the behavior of magnetostrictive transducers as employed in actuator mode. In this paper, the model is applied to magnetostrictive transducers operated in sensor mode. Specifically, the model is used to quantify the magnetization changes exhibited by magnetostrictive materials in response to externally applied forces.

The model is illustrated in the context of the transducer design shown in Figure 1, which is typical of control applications and illustrates the primary components needed to fully utilize the magnetostrictive transducer capabilities. These components are a magnetostrictive rod, an excitation/sensing solenoid which provides the bias magnetization and the sensing voltage $V(t) \propto dB/dt$, a prestress mechanism consisting of a bolt and a spring washer, a permanent magnet which is used in conjunction with the solenoid to fine-tune the bias magnetization, and magnetic couplers.

The model is presented in three stages. In the first stage, we consider the magnetization of the magnetostrictive rod under an externally applied magnetizing field H_0 and a stress field σ. The field-induced component of magnetization is quantified with the mean field model of ferromagnetic hysteresis originally proposed in [15]. The stress-induced component of magnetization is modeled with a law of approach to the anhysteretic magnetization as presented in [16]. The two components considered together provide a magnetization model based on the energy dissipated when domain

walls attach to and detach from inclusions in the material.

The second stage involves the characterization of the magnetostriction λ produced when the magnetostrictive rod is magnetized. This is done through a phenomenological model consisting of an even-terms series expansion depending on M. While λ includes the active contribution to the strain arising from the rotation of magnetic moments, it does not account for the passive or material response of the kind found in ordinary elastic materials and modeled by $s^H \sigma$ in equation (1).

The passive effects are modeled in the third and last stage, through consideration of force balancing in the magnetostrictive rod in the form of a PDE equation which includes the intrinsic magnetostriction, system compliance, internal damping and boundary conditions associated with the mechanical transducer design. The solution to this PDE provides the rod displacements and corresponding total magnetoelastic strain ε.

The accuracy of the model and approximation method are illustrated through comparison of model simulations with experimental data collected from a Terfenol-D sensor.

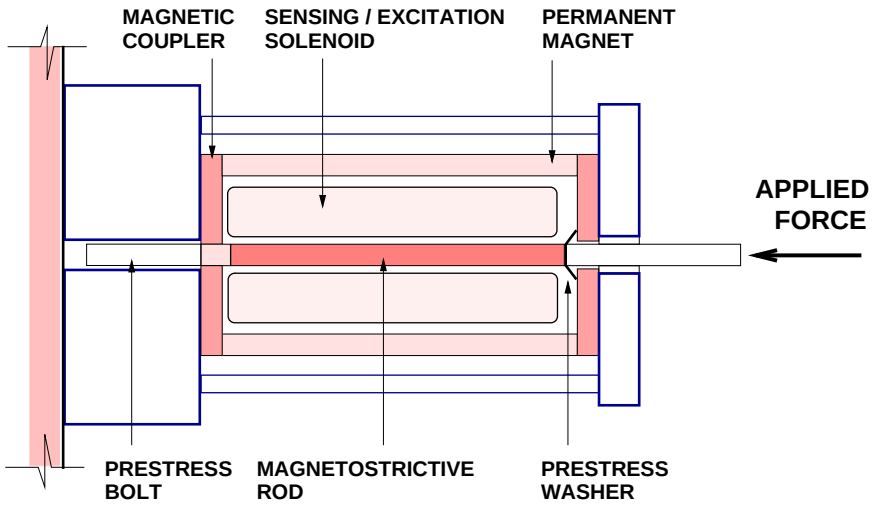

Figure 1: Magnetostrictive sensor used for model development and experimental verification.

MAGNETIZATION OF MAGNETOSTRICTIVE ROD

A magnetomechanical magnetization model was presented in [14] and employed to characterize the magnetization changes which occur in magnetostrictive materials when operated in transducers consisting of an excitation solenoid, a magnetic path and a preload mechanism. The model was constructed on the assumption that the magnetization M is due to a slowly varying magnetic field H and a magnetomechanical component associated with the stresses σ arising as the magnetostrictive material drives or is driven by external loads.

Magnetostrictive transducers are customarily operated under a magnetic bias. This facilitates operation over the region of maximum output per input in the M-H and ε-H curves and leads to bidirectional operation around the bias point. The magnetic bias can be applied via DC currents through the excitation solenoid or with permanent magnets. In order to provide a general model of the performance of biased magnetostrictive sensors, the magnetization changes are assumed to be dictated by the expression

$$\frac{dM}{dt} = \left(\frac{\partial M}{\partial H}\right)\frac{dH}{dt} + \left(\frac{\partial M}{\partial \sigma}\right)\frac{d\sigma}{dt}, \tag{3}$$

where the field contribution arises from the application of a bias magnetization of magnitude H_0 (relative to the demagnetized state) and the stress contribution provides the sensing mechanism.

A domain wall model originally developed by Jiles and Atherton [15] is considered as a basis for characterizing the field effect $\partial M \,/\, \partial H$, while a law of approach to the anhysteretic magnetization is employed to quantify the magnetomechanical effect $\partial M \,/\, \partial \sigma$ [16]. While the time rate of change of magnetic field $dH \,/\, dt$ is readily determined from the rate of application of the magnetic bias H_0, the rate of change of stress $d\sigma \,/\, dt$ must be determined from force balancing in the magnetostrictive rod.

Differential susceptibility. The model for the differential susceptibility $\partial M \,/\, \partial H$ is formulated through consideration of the energy lost when a ferromagnetic material is exposed to a cyclic magnetic field. As the field is applied, magnetic moments in the material rotate into the direction of the field, giving rise to the processes of domain wall motion and domain magnetization rotation [4]. Domains rearrange so as to minimize the total energy, and as a consequence the magnetization changes.

In the idealized case of a defect-free material, on reversal of the field the magnetic moments return to their original orientations and the magnetization returns to its original value. In real engineering materials, however, defects such as crystal imperfections, cracks and voids are typically present which provide pinning sites to which domain walls attach since the total energy is lowest when pinning sites are intersected by a domain wall. For low magnetic field intensities about some equilibrium value, the domain walls remain pinned and bow in a reversible fashion, producing reversible magnetizations. But when the field intensity is sufficiently high so that the magnetic energy overcomes the pinning energy, domain walls detach irreversibly from the pinning sites and attach to remote sites. This mechanism produces energy losses which lead to magnetization hysteresis.

Assuming no other loss mechanisms, the energy supplied to a ferromagnetic material is either converted into magnetostatic energy (total magnetization) or dissipated in the form of irreversible magnetization changes (hysteresis loss due to domain wall pinning). This is formulated through an energy balance in which the total magnetization is calculated from the difference between the maximum attainable magnetization energy, given by the anhysteretic condition, and the energy lost to pinning. The anhysteretic magnetization is calculated using a modified formulation of the Langevin equation [15], while the energy lost to pinning is calculated in terms of a pinning coefficient k that quantifies the density and strength of pinning sites in the material. It is noted that if there is no dissipation, the magnetization must necessarily follow the anhysteretic curve.

We first consider the anhysteretic magnetization M_{an}, which is quantified using the Langevin function $\mathcal{L}(z) \equiv \coth(z) - 1/z$, $-1 < \mathcal{L}(z) < 1$. As detailed in [15], M_{an} has the form

$$M_{an} = M_s \, \mathcal{L}(He/a),$$

in which M_s is the saturation magnetization and the constant a, representing the effective domain density, is treated as a parameter to be estimated through a least squares fit to data or through adaptive parameter identification techniques. The effective magnetic field H_e is found from minimization of a suitable thermodynamic potential, and has the form

$$H_e = H + \alpha \, M + H_\sigma,$$

where H is the applied magnetic field, $\alpha \, M$ is the Weiss interaction field responsible for the alignment of neighboring magnetic moments within domains, and $H_\sigma \equiv 1/\mu_0 \left[\partial \left(\frac{3}{2} \, \sigma \, \varepsilon\right) / \partial M\right]$ is the field due to magnetoelastic interactions.

The differential equations for the irreversible M_{irr} and reversible M_{rev} components of magnetization ($M = M_{rev} + M_{irr}$) in the material can be shown to be [15]

$$M_{irr} = M_{an} - k \, \delta \, \frac{dM_{irr}}{dH_e} \tag{4}$$

$$M_{rev} = c \, (M_{an} - M_{irr}), \tag{5}$$

where parameter δ is +1 when $dH\,/\,dt > 0$ and -1 when $dH\,/\,dt < 0$ to ensure that pinning losses always oppose the magnetization and c is a parameter that quantifies the amount by which domain walls bulge before breaking away from pinning sites.

The total magnetization is then dictated by the superposition of the irreversible and reversible contributions given by equations (4) and (5) respectively,

$$M = M_{irr} + M_{rev} = M_{an} - k\,\delta\,(1-c)\,\frac{dM_{irr}}{dH_e}.$$

This equation leads to the total differential susceptibility $\partial M\,/\,\partial H$ upon differentiation and subsequent application of the chain rule. As detailed in [14], the total differential susceptibility has the form

$$\frac{\partial M}{\partial H} = (1-c)\,\frac{M_{an} - M_{irr}}{\delta\,k - \widetilde{\alpha}(M_{irr},\sigma)\,(M_{an} - M_{irr})} + c\,\frac{\partial M_{an}}{\partial H}. \tag{6}$$

It is noted that in equation (6), the parameter $\widetilde{\alpha}(M_{irr},\sigma)$ represents an effective coupling coefficient which combines the interdomain coupling α and the magnetoelastic interactions,

$$\widetilde{\alpha}(M_{irr},\sigma) = \alpha + \frac{3}{2\,\mu_0}\,\frac{\partial^2(\sigma\,\varepsilon)}{\partial M_{irr}^2}.$$

Magnetomechanical effect. We now consider the contribution of stress to the total magnetization, or magnetomechanical effect $\partial M\,/\,\partial\sigma$. A unifying description of the changes in magnetization due to the action of stress has been recently developed [16]. In the theory presented in [16] and implemented here, the main mechanism governing the magnetomechanical effect is the unpinning of domain walls produced upon application of the stress. On the basis of the key model assumption that hysteresis is originated mainly from domain wall pinning, the freeing of domain walls from their pinning sites must cause the magnetization to change in such a way as to approach the anhysteretic magnetization.

Experimental measurements demonstrate that both the magnitude and the direction of stress-induced magnetization changes are profoundly influenced by the magnetic history of the specimen [16]. It has been observed that the direction in which the magnetization changes with applied stress is independent of the sign of the stress, for small stresses and when the magnetization is sufficiently distant from the anhysteretic. It is then inferred that the direction of change is dependent not on the stress itself, but on a quantity which is independent of the sign of the stress. In this context, it has been hypothesized in [16] that this quantity is the elastic energy per unit volume, $W = \sigma^2/(2E)$, which is clearly independent of the sign of σ. The 'law of approach' to the anhysteretic condition is then formulated as follows: the rate of change of magnetization with elastic energy is proportional to the displacement of the prevailing magnetization from the anhysteretic magnetization, or $\partial M\,/\,\partial W \propto M - M_{an}$. The concept of the law of approach is now applied to the stress-induced magnetization of a magnetostrictive material.

As before, the law of approach may be modeled through irreversible and reversible components of the magnetization. It is noted that to a first approximation, the application of stress produces irreversible magnetization changes since ΔM arising from stress unloading is negligible. Thus, it is reasonable to formulate the law of approach in terms of the irreversible magnetization M_{irr},

$$\frac{\partial M_{irr}}{\partial W} = \frac{1}{\xi}\,(M_{an} - M_{irr}), \tag{7}$$

where ξ is a coefficient with dimensions of energy per unit volume that needs to be identified for magnetostrictive materials. Application of the chain rule $\partial M_{irr}/\partial W = (\partial M_{irr}/\partial\sigma)\,(\partial\sigma/\partial W)$ in

equation (7), along with $\partial W / \partial \sigma = \sigma / E$, yields

$$\frac{\partial M_{irr}}{\partial \sigma} = \frac{\sigma}{E\,\xi}\,(M_{an} - M_{irr}). \tag{8}$$

A similar argument to that used in the field-induced case yields the reversible component,

$$\frac{\partial M_{rev}}{\partial \sigma} = c\,\left(\frac{\partial M_{an}}{\partial \sigma} - \frac{\partial M_{irr}}{\partial \sigma}\right). \tag{9}$$

It is noted that the reversibility coefficient c is the same as that defined in equation (5) because the energy available for domain wall bulging should be independent of the mechanism that produces the bulging, which can be either field- or stress-induced.

Summing the irreversible and reversible contributions given by equations (8) and (9) leads to

$$\frac{\partial M}{\partial \sigma} = (1-c)\,\frac{\sigma}{E\,\xi}\,(M_{an} - M_{irr}) + c\,\frac{\partial M_{an}}{\partial \sigma}, \tag{10}$$

which quantifies the stress-induced magnetization of the magnetostrictive material.

It is noted that on application of stress the magnetization approaches a state of global energy equilibrium. This implies that the anhysteretic magnetization M_{an} must in this case be quantified by iteration of the Langevin function (4) until a solution which satisfies the equation identically is found. Further details regarding the differences between local and global solutions for equation (4) can be found in [14].

ACTIVE COMPONENT OF STRAIN

In order to quantify the contribution of stress to the magnetization given by equation (10), it is necessary to characterize the strain and stress states in the magnetostrictive material. To this end, it is necessary to consider first the deformations which occur in the material when the domain configuration changes. Several models exist for quantifying these deformations, including phenomenological formulations [16], the quadratic law for domain magnetization rotation discussed in [17], energy or thermodynamic formulations [23-25], elastomagnetic models [26-30], micromagnetic theories [18] and magnetization rotation analysis [19]. At low to moderate operating levels, or when material stresses are invariant, these deformations dominate over other material elastic dynamics. In such cases, it is theoretically possible to quantify the bulk magnetostriction upon knowledge of the domain configuration and the magnetostriction along easy crystallographic axes. In the case of Terfenol-D, nominal values for the latter are $\lambda_{111} = 1600 \times 10^{-6}$ and $\lambda_{100} = 90 \times 10^{-6}$, and $\lambda_s \approx 1000 \times 10^{-6}$. In practical terms, however, the domain configuration cannot be known apriori.

To motivate the approach followed here, we consider the particular case when the magnetic field is applied perpendicular to the axis in which the magnetic moments have been aligned by application of sufficiently large compression in the case of a polycrystalline material such as Terfenol-D, or perpendicular to the easy crystallographic axis in a single crystal with uniaxial anisotropy. In either case domain rotation is the prevailing magnetization mechanism, and the magnetostriction along the field direction is given by [17]

$$\lambda(M) = \frac{3}{2}\,\lambda_s \left(\frac{M}{M_s}\right)^2, \tag{11}$$

which predicts a quadratic relation between λ and M. Equation (11) is a single-valued functional, while extensive experimental evidence demonstrates that the λ-M relationship exhibits some degree of hysteresis. For transducer modeling purposes, it is feasible to utilize a single valued λ-M

functional to model the overall shape, and to let M provide the hysteresis through the hysteretic mechanisms in M-H. This approach has proven effective in previous investigations [20].

It should be noted that equation (11) is not sufficiently general when domain wall motion is significant, such as when the operating stress acting on the Terfenol-D material is not extreme ($\sigma_0 < -6.9$ to -20.7 MPa). In order to provide a more general magnetostriction model, we consider a series expansion symmetric about $M = 0$,

$$\lambda(M) = \sum_{i=0}^{\infty} \gamma_i \, M^{2i},$$

in which the coefficients γ_i need to be identified from experimental data. It is noted that quadratic relation (11) is achieved for $i = 1$ with $\gamma_0 = 0$ and $\gamma_1 = (3\,\lambda_s)/(2\,M_s^2)$. For implementation purposes, we consider in this study a quartic law in which the series is truncated after $i = 2$,

$$\lambda(M) = \gamma_1 \, M^2 + \gamma_2 \, M^4. \tag{12}$$

ELASTIC RESPONSE OF THE MAGNETOSTRICTIVE SENSOR

The magnetostriction λ given by equation (12) quantifies the reorientation of magnetic moments towards the direction of applied bias magnetization H_0. It was shown in [13] that this magnetostriction is a generalization of the term $d_{33}H$ in linear models. It ignores, however, the elastic properties of the magnetostrictive material as it vibrates, as represented in the linear models by $s^H\sigma$. In this section, a PDE system is formulated which models the elastic response of the magnetostrictive material and relevant transducer components located in the load path. The input to this PDE is formulated through the magnetostriction λ and the external forces F_{ext} acting on the sensor. The solution to the PDE is the longitudinal displacements $u(t, x)$ relative to the prestressed position.

The structural dynamics are modeled through consideration of the magnetostrictive rod, prestress bolt, prestress washer, and mass load for the transducer in Figure 1. The prestress bolt provides a stress $\sigma_0 < 0$ by compressing the magnetostrictive rod against the washer, modeled by a linear spring k_L and dashpot c_L. The rod is assumed to have length L, cross sectional area A, and longitudinal coordinate x. The material density is ρ, the elastic modulus is E, the internal (Kelvin-Voigt) damping is c_D, and the external load is modeled by a point mass m_L. It should be noted that parameter E lies between the elastic modulus at constant H, E^H, and at constant B, E^B. Since E^H and E^B depend upon the field intensity [21], so does E. However, for simplicity E is treated as a nominal or operational material stiffness.

Assuming linear elasticity and small displacements, force balancing yields the wave equation for the rod vibrations,

$$\rho \, \frac{\partial^2 u}{\partial t^2}(t, x) = \frac{\partial \sigma}{\partial x}(t, x).$$

Here, the stress at cross sections x in the rod is given by [13]

$$\sigma(t, x) = E \, \frac{\partial u}{\partial x}(t, x) + c_D \, \frac{\partial^2 u}{\partial x \partial t}(t, x) - E \, \lambda(t, x) + \sigma_0, \tag{13}$$

where λ is given by (12) and σ_0 is the applied prestress. When integrated over a cross section, equation (13) yields the total inplane resultant N ($N > 0$ in tension, $N < 0$ in compression),

$$N(t, x) = E \, A \, \frac{\partial u}{\partial x}(t, x) + c_D \, A \, \frac{\partial^2 u}{\partial x \partial t}(t, x) - E \, A \, \lambda(t, x) + A \, \sigma_0.$$

To obtain appropriate boundary conditions, it is first noted that at the fixed end of the rod $u(t,x) = 0$. At the end $x = L$, force balancing over an infinitesimal cross section of the rod yields [13]

$$N(t,L) = -m_L \frac{\partial^2 u}{\partial t^2}(t,L) - c_L \frac{\partial u}{\partial t}(t,L) - k_L\, u(t,L) - F_{ext}(t), \tag{14}$$

where F_{ext} is the force applied to the sensor. The negative sign implies that $F_{ext} > 0$ produces a compressive force in the rod.

For implementation purposes, the model is formulated in weak or variational form by multiplying the strong form by test functions ϕ followed by integration throughout the length of the rod. This reduces the smoothness requirements on the finite element basis since displacements and test functions need to be differentiated only once compared to the second derivatives present in the strong form. The space of test functions is $V = H^1_L(0,L) \equiv \{\phi \in H^1(0,L) \mid \phi(0) = 0\}$, so that for all $\phi(x) \in V$,

$$\begin{aligned} \int_0^L \rho\, A \frac{\partial^2 u}{\partial t^2}(t,x)\, \phi(x)\, dx &= -\int_0^L \left[c_D\, A \frac{\partial^2 u}{\partial x \partial t}(t,x) + E\, A \frac{\partial u}{\partial x}(t,x) - E\, A\, \lambda(t,x) \right] \frac{\partial \phi}{\partial x}(x)\, dx \\ &\quad - \left[m_L \frac{\partial^2 u}{\partial t^2}(t,L) + c_L \frac{\partial u}{\partial t}(t,L) + k_L\, u(t,L) + F_{ext}(t) \right] \phi(L). \end{aligned} \tag{15}$$

The solution $u(t,x)$ to this equation defines the longitudinal displacements about the prestressed position and completely defines the elastic state through the strain, given by $\varepsilon(t,x) = \partial u \,/\, \partial x(t,x)$, and the stress $\sigma(t,x)$, given by equation (13).

SUMMARY OF MAGNETOSTRICTIVE SENSOR MODEL

The model under consideration characterizes the behavior of a magnetostrictive sensor in response to two excitations: (i) a bias magnetic field H_0 applied at a known rate $dH \,/\, dt$ and (ii) a stress σ originated from both the externally applied force and the strain produced by the material as it is magnetized. It is emphasized that in this formulation the magnetic and elastic regimes, represented by M and σ respectively, are coupled in accordance with the bidirectional energy transduction process exhibited by magnetostrictive materials. The model addresses both the actuation and sensing regimes by means of a unified mechanism. In actuator mode, externally applied magnetic fields produce magnetization changes which lead to strains and forces produced by the transducer as it drives external loads. In sensor mode, externally applied forces produce magnetization changes in the material which can be detected through the emf created in a sensing coil. The model quantifies the relationship between input and output in either case.

In the presence of a magnetic field H and a stress distribution σ, the magnetization of the magnetostrictive material is dictated by the superposition of the field- and stress-dependent components given by equations (6) and (10),

$$\begin{aligned} \frac{dM}{dt}(t,x) &= \left\{ (1-c)\, \frac{M_{an}(t,x) - M_{irr}(t,x)}{\delta\, k - \widetilde{\alpha}(M_{irr},\sigma)\, (M_{an}(t,x) - M_{irr}(t,x))} + c\, \frac{\partial M_{an}}{\partial H}(t,x) \right\} \frac{dH}{dt}(t,x) \\ &\quad + \left\{ (1-c)\, \frac{\sigma(t,x)}{E\,\xi}\, (M_{an}(t,x) - M_{irr}(t,x)) + c\, \frac{\partial M_{an}}{\partial \sigma}(t,x) \right\} \frac{d\sigma}{dt}(t,x). \end{aligned} \tag{16}$$

To characterize $dH \,/\, dt$, it is necessary to quantify first the quasistatic field $H(t,x)$ generated by the solenoid when a current $I(t)$ circulates through it. To this end, it is often assumed that $H(t) =$ (No. turns /length) $I(t)$. However, this model is only valid in the idealized case of a

lossless, infinitely long solenoid in a lossless magnetic circuit. A more accurate modeling approach consists of identifying H-I by solving numerically Ampère's law or the Biot Savart law, using for instance finite element methods. For purposes of implementing the coupled magnetomechanical model, the approach followed here consisted of determining the H-I relationship experimentally. The corresponding solenoid model is then written in the form,

$$H(t,x) = N_s \, \Psi \, I(t), \tag{17}$$

where N_s is the number of turns in the solenoid and parameter Ψ, which needs to be identified from the experimental data, is a parameter which accounts for solenoid end effects, demagnetizing factors, ohmic losses and flux leakage.

Upon substitution of equation (17) into (16), the final form for the time rate of change of magnetization is determined,

$$\begin{aligned} \frac{dM}{dt}(t,x) &= \left\{ (1-c) \, \frac{M_{an}(t,x) - M_{irr}(t,x)}{\delta \, k - \widetilde{\alpha}(M_{irr},\sigma) \, (M_{an}(t,x) - M_{irr}(t,x))} + c \, \frac{\partial M_{an}}{\partial H}(t,x) \right\} N_s \, \Psi \, \frac{dI}{dt}(t) \\ &+ \left\{ (1-c) \, \frac{\sigma(t,x)}{E \, \xi} \, (M_{an}(t,x) - M_{irr}(t,x)) + c \, \frac{\partial M_{an}}{\partial \sigma}(t,x) \right\} \frac{d\sigma}{dt}(t,x), \end{aligned} \tag{18}$$

which yields $M(t,x)$ upon integration. It should be noted that in the case of constant stress ($d\sigma \,/\, dt = 0$) or constant field ($dI \,/\, dt = 0$), the expression reduces to the individual components characterized by expressions (6) and (10).

After the magnetization $M(t,x)$ arising from the application of $H(t,x)$ and $\sigma(t,x)$ has been identified, the active component of strain is computed from equation (12),

$$\lambda[M(t,x)] = \gamma_1 \, M^2(t,x) + \gamma_2 \, M^4(t,x),$$

where it is noted that since λ depends on the applied magnetic field, it is not homogeneous throughout the rod. Hence, the magnetostriction varies along x.

The longitudinal rod displacements $u(t,x)$ are computed from equation (15)

$$\begin{aligned} \int_0^L \rho \, A \, \frac{\partial^2 u}{\partial t^2}(t,x) \phi(x) \, dx &= - \int_0^L \left[E \, A \, \frac{\partial u}{\partial x}(t,x) + c_D \, A \, \frac{\partial^2 u}{\partial x \partial t}(t,x) - E \, A \, \lambda(t,x) \right] \frac{\partial \phi}{\partial x}(x) \, dx \\ &- \left[F_{ext}(t) + k_L \, u(t,L) + c_L \, \frac{\partial u}{\partial t}(t,L) + m_L \, \frac{\partial^2 u}{\partial t^2}(t,L) \right] \phi(L). \end{aligned}$$

To approximate the solution to this equation, a Galerkin discretization in x is used to reduce the system to a temporal system which is then solved with finite difference approximations. Details regarding the solution method used are provided in [13]. Once the displacements have been characterized, the strain is computed directly using

$$\varepsilon(t,x) = \frac{\partial u}{\partial x}(t,x),$$

and the corresponding stresses acting on the rod are computed directly from the strain using equation (13),

$$\sigma(t,x) = E \, \frac{\partial u}{\partial x}(t,x) + c_D \, \frac{\partial^2 u}{\partial x \partial t}(t,x) - E \, \lambda(t,x) + \sigma_0.$$

It is emphasized that the model was built so that the process $M \Longleftrightarrow \varepsilon \Longleftrightarrow \sigma$ is bidirectional. This means that both the direct effect $M \Longrightarrow \sigma$ and the inverse effect $\sigma \Longrightarrow M$ are treated simultaneously, which is in agreement with the physical considerations discussed in the Introduction.

EXPERIMENTAL VALIDATION

The model summarized in the previous section is now employed to characterize the magnetization changes produced by a Terfenol-D sensor with configuration as illustrated in Figure 1 in response to an externally applied force. The force was generated with a PZT-5A piezoelectric stack and its magnitude was measured with a PCB 086C03 load cell arranged as indicated in Figure 2. The complete device was rigidly clamped to the wall at each end.

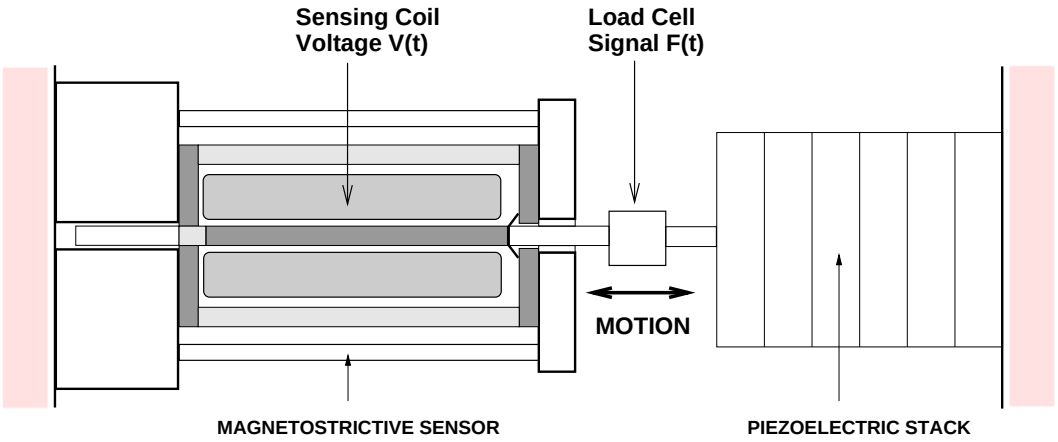

Figure 2: Schematic representation of the assembly used to drive the magnetostrictive sensor. Measured input was driving force $F(t)$, while measured output was sensing voltage $V(t)$.

The measured output from the sensor during operation included sensing voltage $V(t)$ and impressed force $F_{ext}(t)$. The prestress level in the magnetostrictive rod was $\sigma_0 = -3.45$ MPa. A magnetization bias of magnitude $H_0 = 75.8$ kA/m was applied with an Alnico V permanent magnet which was slit longitudinally to reduce eddy current losses. Steel end caps and a Belleville compression washer completed the magnetic circuit.

The magnetostrictive material was a 50 mm long, 6.35 mm diameter monolithic $Tb_{0.3}Dy_{0.7}Fe_{1.92}$ rod manufactured by the Free Stand Zone Melt process. The sensing signal was provided by a 1100-turn solenoid wound with AWG26 magnet wire. The magnetic induction $B_s(t)$ was calculated by integration of the sensing signal $V(t)$. Following the Faraday-Lenz law of magnetic induction, $B_s(t) = -1/(N_s\, A_s) \int_0^t V(\tau)\, d\tau$. Here, A_s is the mean cross sectional area and N_s is the number of turns of the sensing solenoid. Figures 3(a-c) show respectively the 50 Hz applied force, sensing voltage and magnetic induction data obtained in the case of 550 V volts applied to the PZT stack.

For simulation purposes, the material was magnetized by applying a quasistatic (1 Hz) sinusoidal current until the magnetization value H_0 was reached. The current level remained unchanged thereafter to ensure a constant magnetization bias during operation. The magnetic induction was calculated from the model magnetization M and the applied field H via the magnetic constitutive relation $B = \mu_0\,(M + H)$, where μ_0 is the permeability of free space. It is noted that while the derivative $dB\,/\,dt$ provides a characterization of the sensing voltage through $V = -N_s\, A_s\, dB_s\,/\,dt$, derivatives of quantities involving experimental data typically exhibit significant noise, thus precluding a proper comparison of measured and calculated sensing voltages. In this paper, a comparison is established between measured and calculated induction, B_s and B respectively.

The performance of the model is illustrated in Figure 3(d). The model provides a very accurate representation of the magnetic induction in the magnetostrictive rod in both the shape and amplitude of the measured response. The minor phase lag of the model with respect to the data may be explained by eddy current losses in the rod arising due to the 50 Hz frequency of operation.

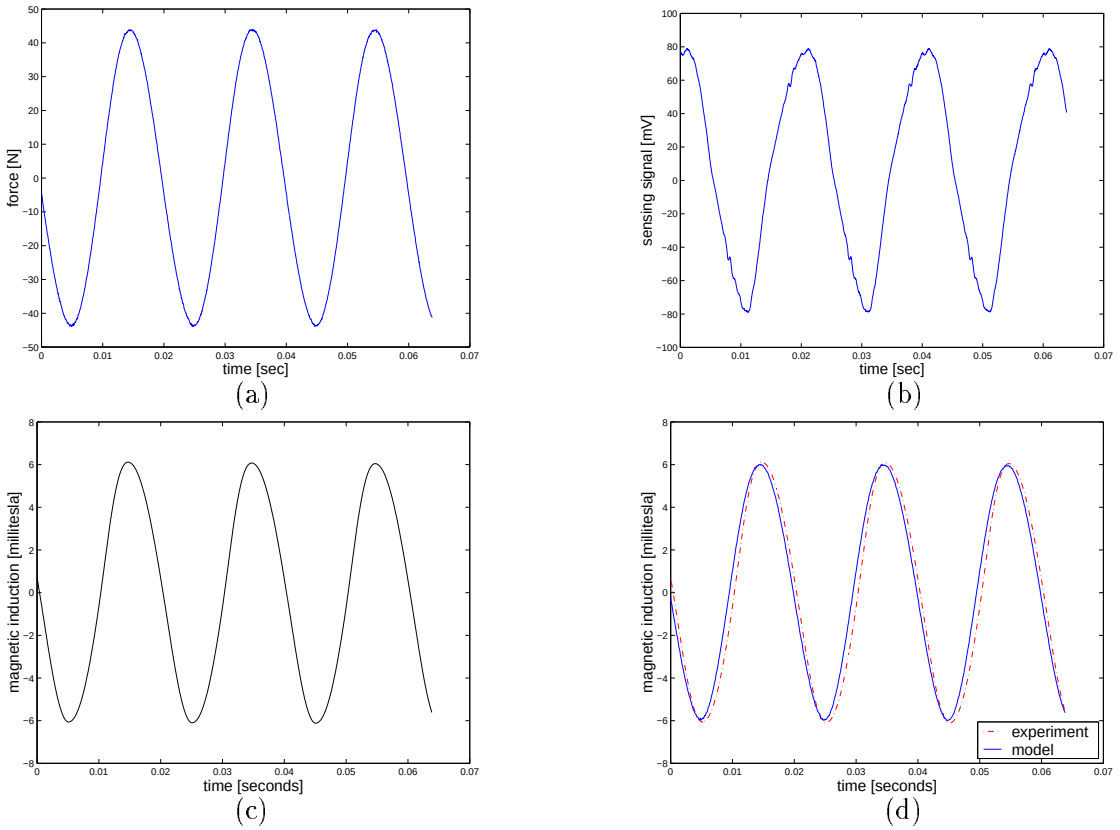

Figure 3: Experimental data: (a) force applied to sensor, (b) sensing voltage from sensor and (c) magnetic induction computed from (b). Model performance: (d) comparison of magnetic induction from model with data shown in (c). The parameters used for model simulation are: $a = 7000$ A/m, $k = 7000$ A/m, $c = 0.2$, $\alpha = 0.065$, $E = 40$ GPa, $\rho = 9250$ Kg/m^3, $\gamma_1 = 2.95 \times 10^{-15}$ m^2/A^2, $\gamma_2 = -6{\times}10^{-28}$ m^4/A^4, $\xi = 8{\times}10^3$ Pa, $c_D = 1{\times}10^6$ Ns/m, $c_L = 1{\times}10^3$ Ns/m, $k_L = 2.66{\times}10^6$ N/m, $m_L = 0.1$ Kg, $\sigma_0 = -3.45$ MPa, $L = 50$ mm, $D = 6.35$ mm.

CONCLUDING REMARKS

A magnetomechanical model for the behavior of magnetostrictive materials as used in sensors has been presented and validated. The model addresses the bidirectional energy transduction between the magnetic and elastic regimes by means of a coupling mechanism which is posed in terms of a PDE system. This PDE system treats indistinctly the case of a magnetostrictive material driving external loads (actuator mode) or being driven by external loads (sensor mode). While some model components are ultimately based on phenomenological observation, crucial aspects of the model are based on thermodynamic principles. In this light, it is expected that a near-constant set of parameters will provide accurate characterization of sensor performance over a wide range of regimes, including the highly nonlinear regimes where prior models provide inaccurate results.

The example demonstrated the use of the model to quantify the magnetic induction changes exhibited by a magnetically biased and mechanically preloaded Terfenol-D rod subjected to external forces. This example provides a template for applications based on magnetostrictive materials in which the induction changes created in a magnetostrictive rod are used to generate voltages in a surrounding sensing coil. It was shown that the model accurately characterizes the relationship between input force and output magnetic induction under low-signal steady state conditions. Work is in progress to evaluate the performance of the model in nonlinear magnetostrictive regimes and to extend the scope of the model by adding transient operation capabilities.

ACKNOWLEDGMENTS

Financial support for M.J.D. and A.B.F. was provided by the NSF Young Investigator Award #CMS9457288 of the Division of Civil and Mechanical Systems. The work of R.C.S. was supported in part by the Air Force Office of Scientific Research under the grant AFOSR F49620-98-1-0180.

REFERENCES

[1] L. Ristic, *Sensor technology and devices* (Artech House, Inc., Norwood, MA, 1994)

[2] F. V. Hunt, *Electroacoustics: the analysis of transduction, and its historical background* (American Institute of Physics for the Acoustical Society of America, 1982)

[3] E. du Trémolet de Lacheisserie, *Magnetostriction theory and applications of magnetoelasticity* (CRC Press, Inc., Boca Raton, FL, 1993)

[4] D. C. Jiles, *Introduction to Magnetism and Magnetic Materials*, (Chapman & Hall, London, 1998)

[5] "Application of the self-sensing principle to a magnetostrictive structural element for vibration suppression," L. Jones and E. Garcia, *ASME Proc. Int. Mech. Eng. Congr. Expos.*, Vol. **45**, pp. 155-165, Chicago (1994)

[6] "Development and analysis of a self-sensing magnetostrictive actuator design," J. Pratt and A. Flatau, *Proceedings of SPIE, Smart Structures and Materials 1993*, Vol. **1917**, p. 952 (1993)

[7] "Passive damping and velocity sensing using magnetostrictive transduction," R. Fenn and M. Gerver, *Proceedings of SPIE, Smart Structures and Materials 1994*, Vol. **2190**, pp. 216-227 (1994)

[8] "Modeling of magnetostrictive sensors," D.K Kleinke and H. M. Uras, *Rev. Sci. Instrum.*, **67**(1), 1996.

[9] "Magnetostrictive torque sensor performance - nonlinear analysis," W. Fleming, *IEEE Trans. Vehic. Tech.*, **38**(3):159-167, August 1989.

[10] "A Terfenol-D based magnetostrictive diode laser magnetometer," R. Chung, R. Weber and D. Jiles, *IEEE Trans. Magn.*, **27**(6):5358-5243, November 1991.

[11] "Spectral estimation for a magnetostrictive magnetic field sensor," J. Doherty, S. Arigapudi and R. Weber, *IEEE Trans. Magn.*, **30**(3):1274-1290, May 1994.

[12] "A coupled structural-magnetic strain model for magnetostrictive transducers," M. J. Dapino, R. C. Smith and A. B. Flatau, *Proceedings of SPIE, Smart Structures and Materials 1999*, Newport Beach, CA (1999)

[13] "A structural-magnetic strain model for magnetostrictive transducers," M. J. Dapino, R. C. Smith and A. B. Flatau, *IEEE Trans. Magn.*, Accepted for publication.

[14] *Nonlinear and hysteretic magnetomechanical model for magnetostrictive transducers*, M. J. Dapino, PhD dissertation, Iowa State University, Ames, Iowa (1999)

[15] "Theory of ferromagnetic hysteresis," D. Jiles and D. Atherton, *J. Magn. Magn. Mater.*, **61**:48–60, 1986.

[16] "Theory of the magnetomechanical effect," D. C. Jiles, *J. Phys. D: Appl. Phys.*, **28**:1537-1546, 1995.

[17] B. D. Cullity, *Introduction to magnetic materials*, (Addison-Wesley, Reading, Massachusetts, 1972)

[18] "Theory of magnetostriction with applications to $Tb_xDy_{1-x}Fe_2$," R. D. James and D. Kinderlehrer, *Philosophical Magazine B*, **68**(2):237-274, 1993.

[19] "Effect of stress on the magnetostriction and magnetization of single crystal $Tb_{0.27}Dy_{0.73}Fe_2$," A. E. Clark, H. T. Savage and M. L. Spano, *IEEE Trans. Magn.*, **MAG-20**(5), 1984.

[20] *Design, analysis and modeling of giant magnetostrictive transducers*, F. T. Calkins, PhD dissertation, Iowa State University, Ames, Iowa (1997)

[21] "Statistical analysis of Terfenol-D material properties," M. J. Dapino, A. B. Flatau and F. T. Calkins, *Proceedings of SPIE, Smart Structures and Materials 1997*, Vol. **3041**, pp. 256-267, San Diego, CA (1997)